Transport in Porous Media (2020) 131:381–397
https://doi.org/10.1007/s11242-019-01347-2

A Coupled Model for Heat and Moisture Transport Simulation in Porous Materials Exposed to Thermal Radiation

Yun Su[1,2,3,4] · Jun Li[3,4] · Xianghui Zhang[3,4]

Received: 14 March 2019 / Accepted: 3 October 2019 / Published online: 1 November 2019

Abstract
Understanding mechanism of transmitted and stored heat in porous materials was extremely important for improving thermal protective performance of clothing. A coupled heat and moisture transfer model in a three-layer fabric system while exposing to a low-level thermal radiation was developed in this study. The model simulated the transmitted and stored heat in porous materials, and considered the effect of moisture transport on the transmitted and stored heat. The predicted results from the coupled model were validated with the experimental results, and compared with the predicted results from the previous model without considering the moisture effect. It was found that the prediction accuracies in skin burn and skin temperature through the coupled model were further improved. The coupled model was used to examine the moisture effect on heat transport and storage in porous materials. The results demonstrated that the moisture within porous materials increased the heat storage and discharge, but decreased the heat transport. The increases in initial moisture content and fiber moisture regain, while increasing the thermal hazardous effect, greatly enhanced the thermal protective performance of clothing. Therefore, it suggested that the moisture management in porous materials was a key consideration for thermal functional design of fabric.

Keywords Porous material · Heat transport · Moisture management · Thermal protection · Heat storage

1 Introduction

Workers in fighting fire and emergency rescue are exposed to thermal hazardous environments, such as high-intensity thermal radiation, flash fire, hot contact, hot liquid and steam

✉ Jun Li
lijun@dhu.edu.cn

Yun Su
swen150@hotmail.com

1 Center for Civil Aviation Composites, Donghua University, Shanghai 201620, China

2 Shanghai Center for High Performance Fibers and Composites, Shanghai 201620, China

3 College of Fashion and Design, Donghua University, Shanghai 200051, China

4 Key Laboratory of Clothing Design and Technology, Ministry of Education, Shanghai 200051, China

(Lee and Barker 1987; Jun et al. 2007; Mandal et al. 2015; Su and Li 2016). Thermal protective clothing as a barrier between the thermal environment and a human body provides a resistance to heat transfer. The clothing with higher thermal protection is typically comprised of a multilayer fabric system (e.g., a shell fabric, a moisture barrier and a thermal liner). However, some recent studies reported that the clothing not only provides the thermal protection but also exerts a thermal hazardous effect on a human body due to the release of stored thermal energy within the clothing (Song et al. 2011a; He et al. 2017; He and He 2017).

In the thermal hazardous environments, the thermal energy penetrating through the thermal protective clothing during heat exposure and stored in the clothing totally determines skin burn injury, since the stored thermal energy could be discharged to the human body after the exposure (Song et al. 2011b). Therefore, the thermal protection provided by the clothing only existed during the exposure. The clothing after the exposure could be seen as a passive heat source that exerted the thermal hazard to the human body. Most studies were conducted to enhance the thermal protective performance, without considering the thermal hazardous effect (Fu et al. 2014; Wang et al. 2012). However, the recent studies showed that most of skin burn injuries were caused from discharging of the stored thermal energy (Song et al. 2011a; He and Li 2016). Thus, it was crucial to investigate the mechanism of the transmitted and stored heat in porous materials for minimizing the thermal hazardous effect.

Several studies were conducted to investigate the stored thermal energy in porous materials. The results demonstrated that the capacity of storing thermal energy was affected by fabric's thickness, density, specific heat and optical properties (Song et al. 2011b; He and Li 2016; Su et al. 2016). For instance, thicker fabric accumulates more thermal energy in high-intensity flame (Song et al. 2011a) and low-level thermal radiation (Song et al. 2011b), and takes longer time to release the thermal stored energy after the exposure (He and Li 2016). The unevenly distributed air gap below the clothing exerted an important effect on the transmitted and stored heat in porous materials (Su et al. 2016; Torvi and Dale 1999). The existence of an air gap, while increasing the heat storage in porous materials, could impede the discharge of stored thermal energy during the cooling (Song et al. 2011a; He and Li 2016). Besides, the stored thermal energy in porous materials presented an increase with the rising of exposure intensity and duration (Song et al. 2011a; Eni 2005). However, there were few studies regarding investigation of moisture effect on the stored thermal energy, let alone to examine how the moisture affects the thermal hazard of the clothing. The moisture contained in the clothing was quite common, and accumulated from sweat, water spray and dew or rains (Mäkinen et al. 1988; Lawson 1997). Some preliminary works demonstrated that the moisture had an important and complicate influence on the thermal protective performance (Barker et al. 2006; Keiser and Rossi 2008). The ignorance of moisture effect on the stored thermal energy was hard to precisely analyze the behavior of heat transfer and thermal storage in porous materials.

However, it was difficult to measure the heat transfer and the thermal energy stored in porous materials and the discharging portion by a laboratory research. Development on numerical models in recent decades provided a possibility for analyzing the transmitted and stored heat in porous materials. Torvi (1997) developed a classic heat transfer model that considered the effect of radiative heat transfer in a single-layer fabric and chemical reaction of fabric in a flash fire. Then, Torvi et al. (2005) further simulated the heat transfer behavior with considering the discharge of stored thermal energy. A clothing model was presented by Song et al. (2004) to study the heat transfer through the clothing during heat exposure and cooling. However, the effect of stored thermal energy on skin burn injury was not analyzed in these models. Recently, Kahn et al. (2012) presented a stored thermal model in a low-intensity

radiation for analyzing the heat storage and release. Then, a compressive heat transfer model was developed to investigate the influence of applied pressure on the stored thermal energy (Su et al. 2016). But there has been no numerical model developed to examine the effect of moisture transport on the transferred and stored heat in porous materials until now.

Therefore, this study aims to develop a heat and moisture transport model in a low-intensity heat exposure for simulating the transferred and stored heat in porous materials. The coupled model is used to analyze the relationships between the transmitted and stored thermal energy. The effects of moisture-related parameters (initial moisture content and fiber moisture regain) on the heat transfer and the heat storage in porous materials are examined. The findings could provide suitable suggestions for improving the thermal protective performance and minimizing the thermal hazardous effect by moisture management in porous materials.

2 Numerical Models

2.1 Effect of Moisture on Heat Transfer

It is known that sensible heat transfer includes thermal conduction, convection and radiation. The convective heat transfer was usually ignored for modeling heat transfer in textile and clothing (Fan et al. 2001). The heat conduction in protective clothing was related to thermo-physical properties of fabric that could be affected by the moisture in porous material. This was because the thermo-physical properties of moisture had a great difference with flame-retardant materials (Prasad et al. 2002). Therefore, the fabric was considered as a multi-phase mixture that consisted of fiber, water in three phases and air. The thermo-physical properties of fabric can be obtained by local volume average theory (Whitaker 1977). Thus, the density (ρ_{fab}), the specific heat ((c_{p})$_{\mathrm{fab}}$), and the thermal conductivity (k_{fab}) of fabric are written as, respectively,

$$\rho_{\mathrm{fab}} = \varepsilon_{\mathrm{bw}}\rho_{\mathrm{bw}} + \varepsilon_{\mathrm{ds}}\rho_{\mathrm{ds}} + \varepsilon_{\mathrm{l}}\rho_{\mathrm{l}} \tag{1}$$

$$(c_{\mathrm{p}})_{\mathrm{fab}} = \frac{\varepsilon_{\mathrm{bw}}\rho_{\mathrm{bw}}(c_{\mathrm{p}})_{\mathrm{bw}} + \varepsilon_{\mathrm{ds}}\rho_{\mathrm{ds}}(c_{\mathrm{p}})_{\mathrm{ds}} + \varepsilon_{\mathrm{l}}\rho_{\mathrm{l}}(c_{\mathrm{p}})_{\mathrm{l}}}{\rho_{\mathrm{fab}}} \tag{2}$$

$$k_{\mathrm{fab}} = \frac{k_{\mathrm{bw}}\rho_{\mathrm{bw}}\varepsilon_{\mathrm{bw}} + k_{\mathrm{ds}}\rho_{\mathrm{ds}}\varepsilon_{\mathrm{ds}} + k_{\mathrm{l}}\rho_{\mathrm{l}}\varepsilon_{\mathrm{l}}}{\rho_{\mathrm{bw}}\varepsilon_{\mathrm{bw}} + \rho_{\mathrm{ds}}\varepsilon_{\mathrm{ds}} + \rho_{\mathrm{l}}\varepsilon_{\mathrm{l}}} \tag{3}$$

where $\varepsilon_{\mathrm{bw}}$, $\varepsilon_{\mathrm{ds}}$ and ε_{l} are the volume percentage of bound water (bw), dry fiber (ds) and liquid water (l), respectively. The gaseous phase in an air filling inter-fiber void space consists of the water vapor and the dry air. The density (ρ_{g}), specific heat ((c_{p})$_{\mathrm{g}}$) and thermal conductivity (k_{g}) of the gaseous phase are given by, respectively,

$$\rho_{\mathrm{g}} = \rho_{\mathrm{v}} + \rho_{\mathrm{a}} \tag{4}$$

$$(c_{\rho})_{\mathrm{g}} = \frac{\rho_{\mathrm{v}}(c_{\rho})_{\mathrm{v}} + \rho_{\mathrm{a}}(c_{\rho})_{\mathrm{a}}}{\rho_{\mathrm{g}}} \tag{5}$$

$$k_{\mathrm{g}} = \frac{k_{\mathrm{v}}\rho_{\mathrm{v}} + k_{\mathrm{a}}\rho_{\mathrm{a}}}{\rho_{\mathrm{v}} + \rho_{\mathrm{a}}} \tag{6}$$

where the subscript v and a are water vapor and dry air, respectively.

Radiative heat transfer in a porous medium was quite complex, involving absorbing, emitting, scattering and transmitting. Beer's law was used to simulate the radiative heat transfer in porous materials. It was defined from the Beer's law that the thermal radiation through porous materials was exponentially decayed due to the material's absorption and

calculated using the transmissivity of porous material (Bergman et al. 2011). The absorbed thermal radiation is calculated by equation,

$$q_{\mathrm{rad}} = q_{\text{rad-incident}}(1 - \exp(-\gamma_{\mathrm{fab}} x)) \tag{7}$$

where γ_{fab} is the extinction coefficient of porous material. The moisture could influence the absorption of thermal radiation in porous materials. Comparing to the absorbed thermal radiation by the liquid water and fiber, the absorption of water vapor and air within the void space could be ignored. Thus, the γ_{fab} is determined by the absorptivity of liquid water (κ_{l}) and fiber (κ_{fib}), given by,

$$\gamma_{\mathrm{fab}} = \kappa_{\mathrm{fib}} + (\varepsilon_{\mathrm{bw}} + \varepsilon_{\mathrm{l}})\frac{\rho_{\mathrm{ds}}}{\rho_{\mathrm{l}}}\kappa_{\mathrm{l}} \tag{8}$$

$$\kappa_{\mathrm{fib}} = \frac{1}{L_{\mathrm{fab}}}\mathrm{In}\left(\frac{1}{1-\alpha_{\mathrm{fib}}}\right) \tag{9}$$

$$\kappa_{\mathrm{l}} = \frac{1}{L_{\mathrm{fab}}}\mathrm{In}\left(\frac{1}{1-\alpha_{\mathrm{l}}}\right) \tag{10}$$

where α_{l} and α_{fib} are the absorptivity of liquid water (0.96) (Modest 2003) and fiber, respectively, and L_{fab} is the fabric thickness.

Additionally, the latent heat exchange of moisture due to phase change and absorption/desorption greatly influenced the heat transfer and thermal storage within porous materials. The enthalpies of evaporation (Δh_{vap}) and transition (Δh_{abs}) from bound water to free liquid, and the mass of transition determined the amount of latent heat exchange. The Δh_{vap} and Δh_{abs} are both dependent on gaseous temperature (T) and relative humidity (Φ), which are obtained by the below equations, respectively (Gibson et al. 1996).

$$\Delta h_{\mathrm{vap}} = 2.792 \times 10^6 - 160T - 3.43T^2 \tag{11}$$

$$\Delta h_{\mathrm{abs}} = 1.95 \times 10^5(1-\phi)\left(\frac{1}{0.2+\phi} + \frac{1}{1.05-\phi}\right) \tag{12}$$

The water evaporation/condensation (m_{vl}) within porous materials was mostly dependent upon vapor concentration and specific surface area of fiber (α_{s}), which is written as,

$$m_{\mathrm{vl}} = h_{\mathrm{m,fab}}\alpha_{\mathrm{s}}\frac{\varepsilon_{\mathrm{l}}}{\varepsilon_{\mathrm{l}}^{\mathrm{cr}}}(\rho_{\mathrm{v}} - \rho_{\mathrm{v,sat}}) \tag{13}$$

where $h_{\mathrm{m,fab}}$ is the convective mass transfer coefficient of water vapor, $\rho_{\mathrm{v,sat}}$ is the concentration of saturated vapor, and $\varepsilon_{\mathrm{l}}^{\mathrm{cr}}$ is the critical value of the liquid fraction at which the liquid phase becomes mobile. When $\rho_{\mathrm{v}} > \rho_{\mathrm{v,sat}}$, $\varepsilon_{\mathrm{l}}^{\mathrm{cr}} = \varepsilon_{\mathrm{l}}$; when $\rho_{\mathrm{v}} \le \rho_{\mathrm{v,sat}}$, $\varepsilon_{\mathrm{l}}^{\mathrm{cr}} = 0.1\varepsilon_{\mathrm{g}}$. The mass transitions from bound water to free liquid water (m_{ls}) and from bound water to water vapor (m_{vs}) can be obtained by the following equations (Gibson and Charmchi 1997), respectively.

$$m_{\mathrm{vs}} = \frac{8D_{\mathrm{f}}\rho_{\mathrm{f}}}{d_{\mathrm{f}}^2}(R_{\mathrm{f,eq}} - R_{\mathrm{f}}) \tag{14}$$

$$m_{\mathrm{ls}} = h_{\mathrm{m}}\alpha_{\mathrm{s}}\gamma_{\mathrm{ls}}\frac{\varepsilon_{\mathrm{l}}}{\varepsilon_{\mathrm{l}}^{\mathrm{cr}}}\left(\frac{R_{\mathrm{f,eq}}}{R_{\mathrm{f}}} - 1\right) \tag{15}$$

where D_{f} is the diffusivity coefficient of the gaseous phase in porous materials, $R_{\mathrm{f,ep}}$ is the equilibrium fiber regain at the fiber surface, R_{f} is the instantaneous fiber regain, γ_{ls} is a

proportionality constant relating to the rate of absorption of liquid water in porous materials. The diffusion coefficient (D_f) is calculated by,

$$D_f = \frac{D_a \varepsilon_g}{\tau} \tag{16}$$

where τ is the fiber tortuosity, and D_a is the diffusion coefficient of air, written as (Song et al. 2008),

$$D_a = 2.23 \times 10^{-5} \left(\frac{T_g}{273.15} \right)^{1.75}. \tag{17}$$

2.2 Heat and Moisture Transfer Equations

In this study, a three-layer fabric system with/without an air gap while exposed to a low-level thermal radiation was simulated. The heat transfer in the fabric system was coupled with the moisture transfer. It was assumed that the heat and moisture transfer was one-dimensional along fabric's thickness. There had no lateral transfer in the fabric system. Volume changes of the fibers due to the variation of moisture content were neglected. There remained the transient thermal equilibrium among the three phases within the fabric system. Thus, the energy conservation equation for each fabric layer is expressed as,

$$(\rho c_\rho)_{\text{fab}} \frac{\partial T}{\partial t} = \frac{\partial}{\partial x} \left(k_{\text{fab}} \frac{\partial \text{T}}{\partial x} \right) + \frac{\partial q_{\text{rad}}}{\partial x} + h_{\text{vap}}(m_{\text{vs}} + m_{\text{vl}}) + h_{\text{abs}}(m_{\text{vs}} + m_{\text{ls}}) \tag{18}$$

where the left side of Eq. (18) represents the accumulative rate of thermal energy in the fabric system. The first term on the right side of Eq. (18) is the conductive heat transfer, the second term on the right side is the radiative heat transfer, the third term on the right side is the contribution due to the phase change of water, and the last term is the change of latent heat due to moisture absorption/desorption.

The convective mass transfer within the void space of fabric driven by Darcian flow was not considered. The water vapor diffusion was mainly driven by the concentration difference in the fabric system. The model ignored the movement of the liquid water due to the resistance of moisture barrier. The transformation of moisture between different phases was driven by phase change and absorption/desorption. Therefore, the continuity equations for the three phases are given by, respectively,

$$\frac{\partial \varepsilon_{\text{bw}} \rho_{\text{bw}}}{\partial t} = m_{\text{vs}} + m_{\text{ls}} \tag{19}$$

$$\frac{\partial \varepsilon_{\text{l}} \rho_{\text{l}}}{\partial t} = m_{\text{vl}} - m_{\text{ls}} \tag{20}$$

$$\frac{\partial (\varepsilon_g \rho_v)}{\partial t} = \frac{\partial}{\partial x} \left(D_f \frac{\partial \rho_v}{\partial x} \right) - m_{\text{vs}} - m_{\text{vl}} \tag{21}$$

where the first term on the left side of Eq. (21) represents the accumulative rate of water vapor in the fabric system. The first term on the right side of Eq. (21) is the molecular diffusion driven by the difference of vapor concentration, and the second and third terms on the right side are both mass transfer rates.

2.3 Initial and Boundary Conditions

The initial temperature and the relative humidity in the porous material were 25° and 65%, respectively. The standard atmosphere pressure was equal to 101.325 kPa. It was supposed

that the initial temperatures of the skin surface and the subcutaneous tissue were, respectively, 32.5° and 37°, and the temperature in different skin depths presented a linear increase along skin thickness. When the porous material was exposed to a radiative heat flux, the outer boundary conditions for the heat and moisture transfer are written as, respectively,

$$-k_{\mathrm{fab}}\frac{\partial \mathrm{T}}{\partial x}|_{x=0} = h_{\mathrm{c,amb}}(T_{\mathrm{amb}} - \mathrm{T}|_{x=0}) + \varepsilon_{\mathrm{fab}}\sigma(T_{\mathrm{amb}}^4 - \mathrm{T}^4|_{x=0}) \tag{22}$$

$$-D_{\mathrm{f}}\frac{\partial \rho_{\mathrm{v}}}{\partial x}|_{x=0} = h_{\mathrm{m,amb}}\left(\rho_{\mathrm{v,amb}} - \rho_{\mathrm{v}}|_{x=0}\right) \tag{23}$$

where $T|_{x=0}$ and T_{amb} are the temperatures of the fabric's outside surface and the surrounding environment, $\rho|_{x=0}$ and $\rho_{\mathrm{v,amb}}$ are the vapor concentrations at the fabric's outside surface and the surrounding environment, and $h_{\mathrm{c,amb}}$ and $h_{\mathrm{m,amb}}$ are the convective heat and mass transfer coefficients between the fabric's outside surface and the surrounding environment, respectively.

The heat transfer from the fabric's inside surface to the skin's surface was determined by heat conduction and phase change. The thermal and moisture boundary conditions at the fabric's inside surface are given by, respectively,

$$-k_{\mathrm{skin}}\frac{\partial T_{\mathrm{s}}}{\partial x}\Big|_{x=L_{\mathrm{fab}}} = -\varepsilon_{\mathrm{g}}k_{\mathrm{g}}\frac{\partial T_{\mathrm{g}}}{\partial x}\Big|_{x=L_{\mathrm{fab}}} - (1-\varepsilon_{\mathrm{g}})k_{\mathrm{s}}\frac{\partial T_{\mathrm{s}}}{\partial x}\Big|_{x=L_{\mathrm{fab}}} + h_{\mathrm{m,air}}\left(\rho_{\mathrm{v}}|_{x=L_{\mathrm{fab}}} - \rho_{\mathrm{v,skin}}\right)h_{\mathrm{vap}} \tag{24}$$

$$-D_{\mathrm{f}}\frac{\partial \rho_{\mathrm{v}}}{\partial x}|_{x=L_{\mathrm{fab}}} = h_{\mathrm{m,air}}\left(\rho_{\mathrm{v}}|_{x=L_{\mathrm{fab}}} - \rho_{\mathrm{v,skin}}\right) \tag{25}$$

where T_{g} and T_{s} are the temperatures of gaseous and solid phases, k_{g} and k_{s} are the thermal conductivities of gaseous and solid phases, $\rho|_{x=L\mathrm{fab}}$ and $\rho_{\mathrm{v,skin}}$ are the vapor concentrations at the fabric's inside surface and the skin's surface, and $h_{\mathrm{m,air}}$ is the convective mass transfer coefficients between the fabric's outside surface and the skin's surface.

3 Numerical Solution

The heat and moisture transfer models were coupled. The heat transfer and mass conservation models of the gaseous phase were both nonlinear partial difference equations, which increased the complexity of calculation. To reduce the calculative errors, the Crank–Nicholson implicit finite difference method was used to discretize these difference equations. The finite difference schemes for the heat transfer and the moisture conservation equations were obtained. Then, the boundary conditions were discretized for obtaining a nonlinear tri-diagonal system. Thomas iterative method was applied to calculate the nonlinear equations (Ozisik 1994). Firstly, the volume percentages of different phases in porous materials were obtained by solving two mass conservation equations of the liquid water and the bound water. Secondly, the mass conservation equation of the gaseous phase was solved to obtain the vapor concentration in porous materials. Based on the calculative results and Eq. (18), the temperature variation in porous materials was solved. The calculative results were required to update these initial conditions and model's input parameters. Thus, the thermal and moisture distribution for the next iteration was calculated. A very fine grid of 1×10^{-5} m was selected for meshing the model's space, while the time step size was set as 0.5 s for improving the precision and stability of predictive results. The program was written in the MATLAB version 9.1.

Table 1 Basic properties of different layer fabrics

Property	Symbol	Unit	OS: 100% Nomex	MB: 80% Nomex/20% Kevlar (PTFE)	TL: 100% M-aramid
Thickness	L	mm	0.6	0.9	2.2
Weight	W	g/m^2	205	110	270
Density	ρ	kg/m^3	342	122	123
Specific heat	c_p	J/kg K	1570	1160	1350
Thermal conductivity	k	W/m K	0.047	0.034	0.035
Fiber volume percentage	ε_{df}	–	0.334	0.186	0.115
Effective tortuosity	τ	–	1.5	1.25	1
Fiber moisture regain at 65% relative humidity	$R_{f,ep}$	–	0.0458	0.0280	0.0597
Diffusion coefficient	D_f	m/s	6×10^{-14}	6×10^{-14}	6×10^{-14}
Proportionality constant related to the rate of absorption of the liquid water	γ_{ls}	–	5×10^{-4}	5×10^{-4}	5×10^{-4}

The standard errors of the experimental test are showed in brackets

4 Results and Discussion

4.1 Model Validation

The presented model was validated with the experimental results reported by Su et al. (2016). The three-layer fabric system including an outer shell (OS), a moisture barrier (MB) and a thermal liner (TL) was selected in the experiment. The basic properties of different layer fabrics are listed in Table 1. The three-layer fabric system was preconditioned in a chamber of 25 °C temperature and 65% relative humidity for 24 h, and then was exposed to a 8.5 kW/m^2 radiative heat flux for 300 s. A 6.4-mm spacer was introduced between the fabric system and the sensor for simulating an air gap below clothing. After the exposure, the thermal response on the sensor was measured unceasingly for 200 s. The skin temperatures and the times to cause skin burn were both obtained by the experiment for verifying the presented model.

4.1.1 Comparison of Burn Time

Table 2 presents the experimental results of times to cause second- and third-degree burn and the standard errors. The predicted results by the previous model (Su et al. 2016) and the current model were compared, and showing their relative errors with the experiment. It was found that the skin burn times predicted by the previous model were less than that of the experimental test, while most of the skin burn times predicted by the current model were greater than the experiment (except for third-degree burn with 6.4 mm air gap). The reason might be that the heat transfer considering the moisture effect increased the stored

Table 2 Experimental and predicted results of times to second- and third-degree burns

	Time to second-degree burn		Time to third-degree burn	
	0 mm	6.4 mm	0 mm	6.4 mm
Experiment, t_1(s)	103.4 (3.87)	163.8 (2.02)	159.3 (6.48)	287.5 (4.09)
Previous model, t_2(s)	83.5	146.8	130.5	264.2
Current model, t_3(s)	122.6	166.0	187.0	253.4
Previous model, $\lvert t_2 - t_1 \rvert / t_1$	19.24%	9.95%	18.07%	10.43%
Current model, $\lvert t_3 - t_1 \rvert / t_1$	18.57%	1.34%	17.39%	11.86%

thermal energy in the fabric system, thus slowing down the time to cause skin burn (Kukuck and Prasad 2003). However, the moisture within the clothing could increase the heat transfer rate due to higher thermal conductivity after the ceasing of storing thermal energy (Su et al. 2017). Thus, the time to cause third-degree burn predicted by the current model was less than the experiment. In addition, the relative errors of the current model for no air gap were slightly less than the previous model. This indicated that the coupled model on the heat and moisture transfer predicted more precisely skin burn injuries under no air gap. For the existence of the air gap, the relative errors of the times to second- and third-degree burn presented a great difference, but the average error for the current model was less than the previous model. Therefore, the current model was capable of predicting the skin burn injury under the low-level thermal radiative exposure.

4.1.2 Comparison of Skin Temperature

For further validating the reliability of the current model, Fig. 1 shows the skin temperature from the experimental measurement and these model predictions. The experimental process included two periods: (a) an increasing period during the heat exposure; (b) a decreasing period during the cooling. A good agreement between the experimental measurement and these model predictions was observed for both periods. For the current model, the predicted skin temperature under the air gap was lower firstly and then higher than the experimental results. The predicted deviation reached a peak during the cooling. However, the skin temperature predicted by the current model under no air gap was lower than the experimental results, but presented a higher consistence with the experiment. This indicated that the predicted heat transfer rate in the air gap was higher than the experimental test. The reason might be attributed to the ignorance of multi-dimensional heat and moisture transfer in the porous material.

Figure 1 also demonstrated some discrepancies in the predicted skin temperature between two models. The predicted skin temperature by the current model was greatly lower than the previous model, which showed similar results with the experimental test under dry and wet conditions (Song et al. 2011b). For the previous model, the predictive deviation increased gradually during the heat exposure. The highest deviations without and with the air gap were around 2.93° and 1.59°, respectively. The predictive deviations for the current model without and with the air gap were around 2.05° and 2.66°, respectively. This indicated that the skin temperature predicted by the current model under no air gap was closer to the experimental results. That is to say, the heat and moisture transfer model in the porous material presented better predicted results. However, the predicted error under the air gap had no decrease

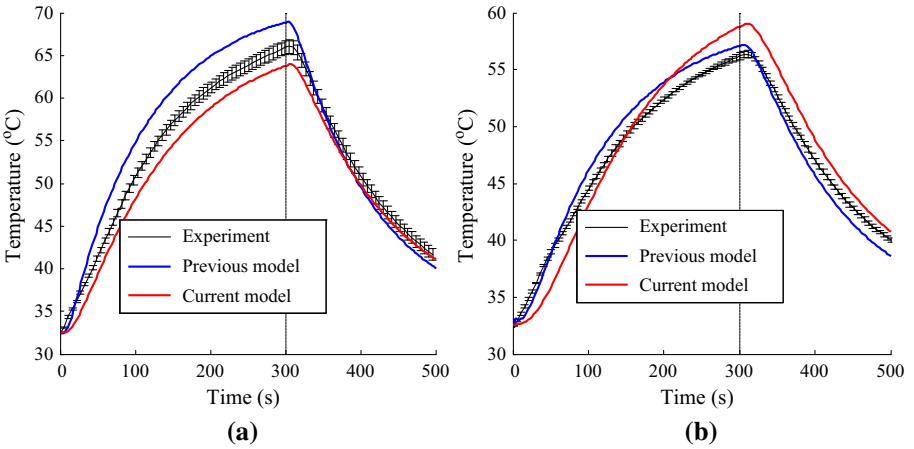

Fig. 1 Measured and predicted skin temperature responses for multilayer protective clothing **a** without an air gap and **b** with an air gap

comparing to the previous model, indicating that the heat and moisture transfer in an air gap was required to be further improved.

4.2 Relationships Between Transmitted and Stored Thermal Energy

Understanding the mechanisms of heat transfer and heat storage in a porous material was extremely important for improving the thermal protection and reducing the thermal hazard. Although the relationships between heat transfer and heat storage were investigated in the previous studies, these studies did not consider the moisture effect on heat transfer and heat storage (He et al. 2017; Su et al. 2016). This could incorrectly reflect the variation of heat storage and heat release. Therefore, the current model was employed to analyze the changes of the transmitted and stored thermal energy, and was compared to the results predicted by the previous model (Su et al. 2016).

The storing and transmitting energy rates for each-layer fabric in wet and dry heat transfer are shown in Fig. 2a, b. Significant differences between wet and dry heat transfer were observed for the transmitted and stored energy rates of each-layer fabric. This implied that the moisture affected the behavior of the transmitted and stored thermal energy in the porous material. The presence of moisture effect increased heat storage and decreased transmitted heat, which was consistent with the experimental results of Song et al. (2011b) under a low-level thermal radiation. Thus, the moisture could increase the thermal hazardous effect of clothing.

For the storing energy rate, it was clear that the peak values for each-layer fabric under wet heat transfer were both larger than that under dry heat transfer. The existence of moisture enhanced the storing energy rate. Besides, the storing energy rate under dry heat transfer took shorter times to arrive to a stable state (before 100 s). However, the storing energy rate under wet heat transfer reaching to the stable state was after the exposure of 200 s. This indicated that the porous material under wet heat transfer stored more thermal energy. This was due to the fact that the moisture replacing the air in the void space of the fabric increased the capacity of storing thermal energy. As shown in Table 3, the stored thermal energy ($Q_{\text{s-dry}}$) for the outer shell, the moisture barrier and the thermal liner under dry heat transfer were 73.20,

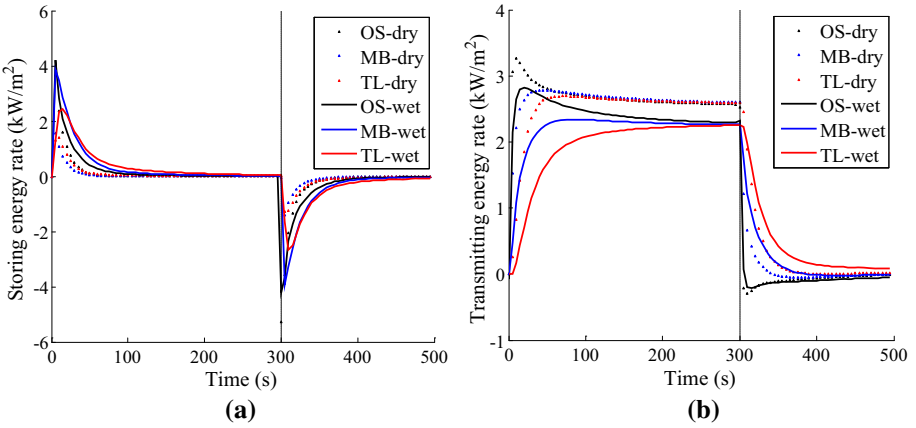

Fig. 2 Transmitting and storing energy rates for each-layer fabric without an air gap

Table 3 Storing, discharging and transmitting thermal energy for each-layer fabric

	Outer shell: OS	Moisture barrier: MB	Thermal liner: TL
$Q_{s\text{-dry}}$ (kJ/m^2)	73.20	29.19	37.29
$Q_{s\text{-wet}}$ (kJ/m^2)	108.46	128.18	126.77
$Q_{d\text{-dry}}$ (kJ/m^2)	72.98	29.02	36.93
$Q_{d\text{-wet}}$ (kJ/m^2)	97.22	113.72	107.23
$Q_{t\text{-exp-dry}}$ (kJ/m^2)	806.98	786.03	750.95
$Q_{t\text{-exp-wet}}$ (kJ/m^2)	764.51	655.52	580.64
$Q_{t\text{-cool-dry}}$ (kJ/m^2)	− 12.69	16.80	53.44
$Q_{t\text{-cool-wet}}$ (kJ/m^2)	− 14.85	38.36	83.83

$Q_{s\text{-dry}}$ and $Q_{s\text{-wet}}$, stored thermal energy under dry and wet heat transfer, respectively; $Q_{d\text{-dry}}$ and $Q_{d\text{-wet}}$, discharged thermal energy under dry and wet heat transfer, respectively; $Q_{t\text{-exp-dry}}$ and $Q_{t\text{-exp-wet}}$, transmitted thermal energy during the exposure under dry and wet heat transfer, respectively; $Q_{t\text{-cool-dry}}$ and $Q_{t\text{-cool-wet}}$, are transmitted thermal energy during the cooling under dry and wet heat transfer, respectively

29.19 and 37.29 kJ/m^2, respectively. The stored thermal energy ($Q_{s\text{-wet}}$) for the three-layer fabrics under wet heat transfer increased to 108.46, 128.18 and 126.77 kJ/m^2, respectively. The reason why the stored thermal energy for the moisture barrier and the thermal liner presented greater growth rate was because the moisture barrier and the thermal liner have larger void percentage to store moisture (see Table 1).

After the exposure, the storing energy rate was less than zero, meaning that the stored thermal energy started to release. There had a greater rate to discharge thermal energy under wet heat transfer. Likewise, more thermal energy under wet heat transfer was discharged to the surrounding environment and the human body. The storing energy rates for wet and dry heat transfer at the end of cool down were both close to zero, which indicated a ceasing of heat discharge. A new index (efficiency of heat discharge) was proposed by dividing total discharge energy (Q_d) by total stored energy (Q_s). The efficiencies of heat discharge under dry heat transfer were 99.70%, 99.42% and 99.03%, respectively, for the outer shell, the moisture barrier and the thermal liner. The heat discharge efficiencies for the three-layer

fabrics under wet heat transfer were 89.64%, 88.71% and 84.59%, respectively. Thus, the moisture transport decreased the heat discharge efficiency.

The changes in the transmitting energy rate under dry and wet heat transfer are shown in Fig. 2b. Generally, the transmitting energy rate during the exposure was decreased greatly while considering the moisture effect. Besides, the difference of total transmitting energy between wet and dry heat transfers presented an increase from the outer-layer fabric to the inner-layer fabric (see Table 3). The reason might be that the transmitting thermal energy was stored not only by the porous material, but also by the moisture within the void space. However, there was an increase in the transmitting energy rate during the cooling under wet heat transfer. This was because the transmitting energy rate during the cooling was strongly determined by the amount of stored thermal energy. Additionally, the transmitting energy rates of the outer shell and the moisture barrier during the cooling were negative value, since these fabrics released the thermal energy to the external environment. As shown in Table 3, the transmitting energy to the external environment and the human body under wet heat transfer was larger than that under dry heat transfer. The transmitting energy to the external environment included the discharging energy from the outer shell and the heat transfer from the inner layer to the outer shell. The values under dry and wet heat transfer were 85.67 and 112.07 kJ/m^2, respectively. Therefore, more stored thermal energy after the exposure was transferred to the external environment under wet heat transfer.

4.3 Effect of Moisture on Transmitted and Stored Thermal Energy

The presence of moisture within the porous material influenced greatly the transmitted and stored thermal energy. However, the moisture effect on the thermal protective performance of the porous material was dependent on various factors, such as moisture distribution, moisture content and fiber moisture absorption. Therefore, the current model was used to simulate heat and moisture transfer in a porous material without an air gap while exposing to a low-level thermal radiation (8.5 kW/m^2). This would further investigate the effects of initial moisture content and fiber moisture regain on the transmitted and stored thermal energy.

4.3.1 Effect of Initial Moisture Content

Figure 3 depicts changes in total storing and total transmitting energy rates with the initial moisture content. The storing and transmitting energy rates both showed obvious difference between different initial moisture contents. The maximum storing energy rate decreased over an increase in initial moisture content. This was because the addition of liquid water raised the heat transfer rate in the porous material. However, the shortest time for storing thermal energy was the thermal liner without the initial moisture content, meaning that the addition of liquid water prolonged the time for storing thermal energy. At the end of the heat exposure, the porous material containing liquid water still retained the capacity for storing thermal energy. Due to the limitation of the heat exposure duration, the total stored thermal energy during the exposure showed a slight decrease with the initial moisture content. After the exposure, there had a small difference for the heat discharging rate between different initial moisture contents. A positive relationship between the heat discharging rate and the total stored thermal energy was observed, indicating that the rising of stored thermal energy could improve the heat discharging rate.

For the transmitting energy rate, the addition of liquid water presented a significant effect during the exposure. Without the adding liquid water, the transmitting energy rate firstly

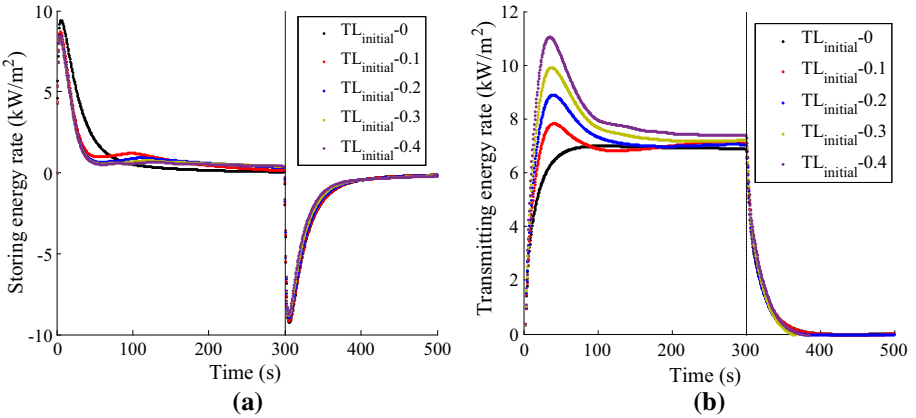

Fig. 3 Effect of initial moisture content on **a** storing and **b** transmitting energy rates

increased and then reached a stable state. However, the transmitting energy rate climbed up, then declined, and finally achieved stability when liquid water was added to the thermal liner before the exposure. There existed peak values for the transmitting energy rate with the addition of liquid water, which showed an increasing trend with the initial moisture content. Besides, the ultimate rate of transmitting energy after ceasing the exposure increased versus the initial moisture content, since the thermal conductivity of liquid water is far larger than most of the flame-resistant materials (Prasad et al. 2002). The transmitting energy rate after the exposure had no obvious difference, which was determined by the total stored thermal energy.

The effects of initial moisture content on the thermal protection and the thermal hazard could be examined by using the absorbed thermal energy by skin during the exposure and the cooling, respectively, as shown in Fig. 4. Fitting analysis was carried out to obtain the variation tendency of thermal energy during the exposure and the cooling. In general, the moisture addition contributed to the decrease in the absorbed thermal energy, which means the rising of thermal protection and the decrease in thermal hazard. The declining rate was larger for the thermal energy during the exposure, indicating that the influence of moisture addition on the thermal protection was more significant than the thermal hazard. However, the further increase in moisture content did not improve the thermal protection and decrease the thermal hazard. The porous material with the initial moisture content of 20% provided the highest thermal protection, and the lowest thermal hazard exerted by the porous material was when the initial moisture content was 30%. The reason might be due to the combined effects contributed by increases in the stored thermal energy and conductive heat transfer with the addition of moisture content (Song et al. 2011a; Prasad et al. 2002). The changing trend of the thermal protection was also proved by other studies (Barker et al. 2006; Su et al. 2017). Additionally, it was clear that the absorbed thermal energy during the cooling was less than 20% of the absorbed thermal energy during the exposure. This signified that the thermal hazardous effect was relatively small for 300 s exposure and 200 s cooling.

Table 4 shows the effects of initial moisture content on times to second- and third-degree skin burns. It was found that the skin burn times presented a firstly increase and then decrease with the initial moisture content. The contributions of the thermal protection and the thermal hazard on skin burn injury were further examined by correlation analysis between the absorbed thermal energy and the skin burn time (significant level = 0.05). The results showed

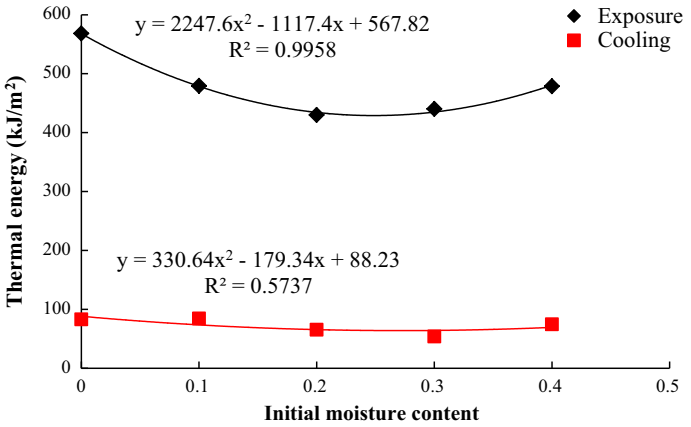

Fig. 4 Effects of initial moisture content on thermal protection and thermal hazard

Table 4 Times to second- and third-degree burns with the initial moisture content

Initial moisture content	Time to second-degree burn (s)	Time to third-degree burn (s)
0	122.6	187.0
0.1	173.0	237.5
0.2	186.0	265.0
0.3	174.0	263.0
0.4	150.0	241.5

that the absorbed thermal energy during the exposure and the cooling both presented a negative correlation with the times to second- and third-degree skin burns. However, the *P* value of less than 0.05 was only found for the absorbed thermal energy during the exposure. Therefore, the skin burn injury was mostly caused by the absorbed thermal energy during the exposure.

4.3.2 Effect of Fiber Moisture Regain

The effects of fiber moisture regain on total storing and total transmitting energy rates are shown in Fig. 5. It was obvious that the porous material with excellent moisture absorption demonstrated a low rate of storing thermal energy. With the further increase in exposure time, the storing energy rate decreased sharply. Also, the storing energy rate for higher moisture absorption was greater gradually than that for lower moisture absorption. The total thermal storage presented a decrease with the rising of fiber moisture regain. The maximum difference for the total thermal storage reached to 16.96 kJ/m^2.

As shown in Fig. 5b, the transmitting energy rate increased rapidly and gradually remained an equilibration during the exposure. The increase in fiber moisture regain slightly enhanced the transmitting energy rate. There was a growth in the total transmitting energy over the fiber moisture regain. This was because the conductive heat transfer could be enhanced if the porous material provided excellent moisture absorption. The biggest difference of the total transmitting energy was 38.97 kJ/m^2. During the cooling, there had no obvious difference in the storing energy rate between different fiber moisture regains. But the total thermal discharge decreased with the fiber moisture regain. The maximum difference for the

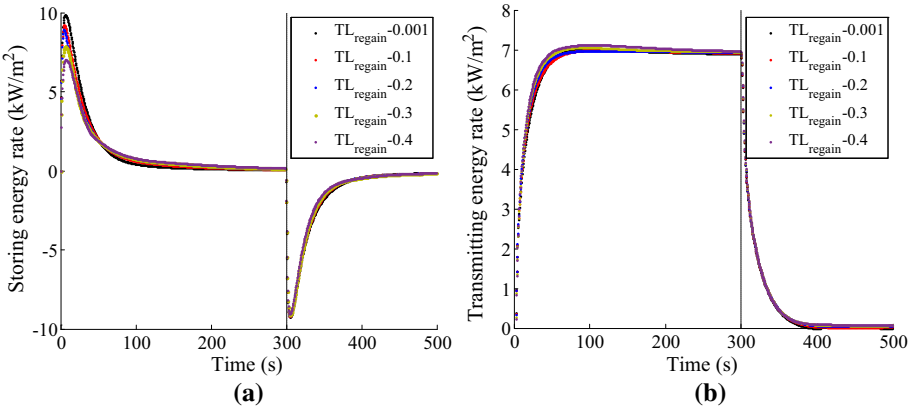

Fig. 5 Effects of fiber moisture regain on **a** storing and **b** transmitting energy rates

total thermal discharge was 24.70 kJ/m^2. Thus, the porous material with excellent moisture absorption diminished the discharge from the stored thermal energy.

The absorbed thermal energy by skin during the exposure and the cooling was used to evaluate the effect of the fiber moisture regain on the thermal protection and the thermal hazard (see Fig. 6). It was clear that a linear relation between the absorbed thermal energy, and the fiber moisture regain was observed. The determination coefficients (R^2) for the exposure and the cooling were both larger than 0.9. The rising of the fiber moisture regain decreased the absorbed thermal energy during the exposure, but increased the absorbed thermal energy during the cooling. This indicated that the rising of fiber moisture regain, while enhancing the thermal protection, increased the thermal hazard caused by the porous material. Additionally, the fitting equations demonstrated that the fiber moisture regain presented a greater influence on the thermal protection. Thus, the increase in the fiber moisture regain tended to increase the thermal protective performance. However, the percentage that the absorbed thermal energy during the cooling accounts for the absorbed thermal energy during the exposure markedly increased with the fiber moisture regain. The percentage for the fiber moisture regain of 0.4 was approximately 24.2%. It was indicated that the thermal hazardous effect was more significant with the fiber moisture regain.

Table 5 lists the times to cause second- and third-degree burns under different fiber moisture regains. The times to cause second- and third-degree burns both showed an increase over the fiber moisture regain. The porous material with excellent moisture absorption provided higher thermal protective performance for reducing the second- and third-degree burns. The absorbed thermal energy during the exposure presented a highly negative correlation with the times to cause second- and third-degree burns ($r_{2nd} = -0.999$, $r_{3rd} = -0.998$). This was because the skin burns were caused in 300 s exposure. Therefore, the skin burns in the low-level thermal radiation for 300 s exposure was determined by the absorbed thermal energy during the exposure.

5 Conclusions

A coupled heat and moisture transfer model was developed for analyzing the moisture effect on the transmitted and stored thermal energy in porous materials under a low-level thermal radiation. The current model considered the effect of moisture on heat conduction, thermal

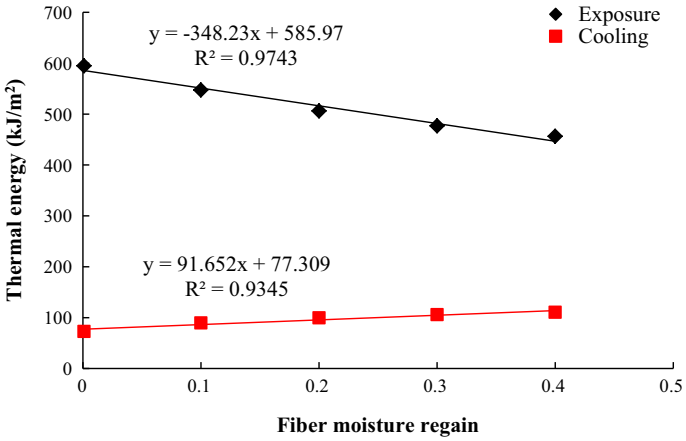

Fig. 6 Effects of fiber moisture regain on thermal protection and thermal hazard

Table 5 Times to second- and third-degree burns with the fiber moisture regain

Fiber moisture regain	Time to second-degree burn (s)	Time to third-degree burn (s)
0.001	111.0	172.0
0.1	131.5	198.0
0.2	148.5	220.5
0.3	160.0	234.0
0.4	167.0	242.0

radiation and heat storage in porous materials. The finite difference method was employed to resolve the mathematical model. The predicted results by the current model under no air gap presented a higher consistence with the experimental results comparing to the simulated results without considering the moisture transport.

The improved model was further used to investigate the relationship between the transmitted and stored heat in porous materials, and the effects of initial moisture content and fiber moisture regain. It was found that the moisture transport, while declining the heat transport in porous materials, increased the heat storage and the heat discharge. The thermal hazardous effect caused by protective clothing was enhanced by the moisture transport. In addition, the initial moisture content and the fiber moisture regain both exerted significant effects on the thermal protective performance and the thermal hazard. Therefore, it was crucial for improving the thermal protective performance of protective clothing by studying the moisture management in porous materials.

Funding This work was sponsored by Shanghai Sailing Program, Open Fund of Shanghai Center for High Performance Fibers and Composites, and Fundamental Research Funds for the Central Universities (Grant NO. 2232019G-08).

References

Barker, R., Guerth, C., Behnke, W., Bender, M.: Measuring the thermal energy stored in firefighter protective clothing. ASTM Spec. Tech. Publ. **1386**, 33–44 (2000)

Barker, R.L., Guerth-Schacher, C., Grimes, R., Hamouda, H.: Effects of moisture on the thermal protective performance of firefighter protective clothing in low-level radiant heat exposures. Text. Res. J. **76**(1), 27–31 (2006)

Barker, R.L., Deaton, A.S., Ross, K.A.: Heat transmission and thermal energy storage in firefighter turnout suit materials. Fire Technol. **47**(3), 549–563 (2011)

Bergman, T.L., Incropera, F.P., Lavine, A.S.: Fundamentals of Heat and Mass Transfer. Wiley, New York (2011)

Eni, E.U.: Developing test procedures for measuring stored thermal energy in firefighter protective clothing (2005)

Fan, J.T., Luo, Z.X., Li, Y.: Heat and moisture transfer with sorption and condensation in porous clothing assemblies and numerical simulation (vol 43, pp 2989, 2000). Int. J. Heat Mass Transf. **44**(5), 1079–1079 (2001)

Fu, M., Weng, W.G., Yuan, H.Y.: Quantitative assessment of the relationship between radiant heat exposure and protective performance of multilayer thermal protective clothing during dry and wet conditions. J. Hazard. Mater. **276**(9), 383–392 (2014)

Gibson, P.: Multiphase heat and mass transfer through hygroscopic porous media with applications to clothing materials, DTIC Document (1996)

Gibson, P.W., Charmchi, M.: Modeling convection/diffusion processes in porous textiles with inclusion of humidity-dependent air permeability. Int. Commun. Heat Mass **24**(5), 709–724 (1997)

He, J., He, J.: Quantitative assessment of the thermal stored energy in protective clothing under low-level radiant heat exposure. Text. Res. J. **88**, 2867–2879 (2017)

He, J., Li, J.: Analyzing the transmitted and stored energy through multilayer protective fabric systems with various heat exposure time. Text. Res. J. **86**(3), 235–244 (2016)

He, J., Lu, Y., Chen, Y., Li, J.: Investigation of the thermal hazardous effect of protective clothing caused by stored energy discharge. J. Hazard. Mater. **338**, 76–84 (2017)

Jensen, R.L.J.: Thermal performance of firefighters' protective clothing. Paper Provided to Industry, 3M, Minneapolis (1998)

Li, J., Barker, R.L., Deaton, A.S.: Evaluating the effects of material component and design feature on heat transfer in firefighter turnout clothing by a sweating Manikin. Text. Res. J. **77**(2), 59–66 (2007)

Kahn, S.A., Patel, J.H., Lentz, C.W., Bell, D.E.: Firefighter burn injuries: predictable patterns influenced by turnout gear. J. Burn Care Res. **33**(1), 152–156 (2012)

Keiser, C., Rossi, R.M.: Temperature analysis for the prediction of steam formation and transfer in multilayer thermal protective clothing at low level thermal radiation. Text. Res. J. **78**(11), 1025–1035 (2008)

Kukuck, S., Prasad, K.: Thermal Performance of Fire Fighters' Protective Clothing. 3. Simulating a TPP Test for Single-Layered Fabrics, National Institute of Standards and Technology, Gaithersburg, MD (2003)

Lawson, J.R.: Fire fighters' protective clothing and thermal environments of structural fire fighting. ASTM Spec. Tech. Publ. **1273**, 334–335 (1997)

Lee, Y.M., Barker, R.L.: Effect of moisture on the thermal protective performance of heat-resistant fabrics. J. Fire Sci. **4**(5), 315–331 (1986)

Lee, Y.M., Barker, R.L.: Thermal protective performance of heat-resistant fabrics in various high intensity heat exposures. Text. Res. J. **57**(3), 123–132 (1987)

Mäkinen, H., Smolander, J. Vuorinen, H.: Simulation of the effect of moisture content in underwear and on the skin surface on steam burns of fire fighters. In: Performance of Protective Clothing: Second Symposium, ASTM STP, pp. 415–421 (1988)

Mandal, S., Song, G., Gholamreza, F.: A novel protocol to characterize the thermal protective performance of fabrics in hot-water exposure. J. Ind. Text. **46**, 279–291 (2015)

Modest, M.F.: Radiative Heat Transfer, 2nd edn. Academic Press, Amsterdam (2003)

Ozisik, N.: Finite Difference Methods in Heat Transfer. CRC Press, Boca Raton (1994)

Prasad, K., Twilley, W.H., Lawson, J.R.: Thermal performance of fire fighters' protective clothing: numerical study of transient heat and water vapor transfer, US Department of Commerce, Technology Administration, National Institute of Standards and Technology (2002)

Song, G., Barker, R.L., Hamouda, H., Kuznetsov, A.V., Chitrphiromsri, P., Grimes, R.V.: Modeling the thermal protective performance of heat resistant garments in flash fire exposures. Text. Res. J. **74**(12), 1033–1040 (2004)

Song, G., Chitrphiromsri, P., Ding, D.: Numerical simulations of heat and moisture transport in thermal protective clothing under flash fire conditions. Int. J. Occup. Saf. Ergo. **14**(1), 89–106 (2008)

Song, G., Gholamreza, F., Cao, W.: Analyzing stored thermal energy and thermal protective performance of clothing. Text. Res. J. **81**(11), 1124–1138 (2011a)
Song, G., Paskaluk, S., Sati, R., Crown, E.M., Dale, J., Ackerman, M.: Thermal protective performance of protective clothing used for low radiant heat protection. Text. Res. J. **81**(3), 311–323 (2011b)
Su, Y., Li, J.: Development of a test device to characterize thermal protective performance of fabrics against hot steam and thermal radiation. Measur. Sci. Technol. **27**(12), 125904 (2016)
Su, Y., He, J., Li, J.: An improved model to analyze radiative heat transfer in flame-resistant fabrics exposed to low-level radiation. Text. Res. J. **87**, 1953–1967 (2016a)
Su, Y., He, J., Li, J.: Modeling the transmitted and stored energy in multilayer protective clothing under low-level radiant exposure. Appl. Therm. Eng. **93**, 1295–1303 (2016b)
Su, Y., He, J., Li, J.: A model of heat transfer in firefighting protective clothing during compression after radiant heat exposure. J. Ind. Text. **47**, 2128–2152 (2016c)
Su, Y., Li, J., Song, G.: The effect of moisture content within multilayer protective clothing on protection from radiation and steam. Int. J. Occup. Saf. Ergo. **24**, 1–10 (2017)
Torvi, D.A.: Heat transfer in thin fibrous materials under high heat flux conditions, University of Alberta (1997)
Torvi, D.A., Dale, J.D.: Heat transfer in thin fibrous materials under high heat flux. Fire Technol. **35**(3), 210–231 (1999)
Torvi, D.A., Eng, P., Threlfall, T.G.: Heat transfer model of flame resistant fabrics during cooling after exposure to fire. Fire Technol. **42**(1), 27–48 (2005)
Wang, Y.-Y., Lu, Y.-H., Li, J., Pan, J.-H.: Effects of air gap entrapped in multilayer fabrics and moisture on thermal protective performance. Fibers Polym. **13**(5), 647–652 (2012)
Whitaker, S.: Simultaneous heat, mass, and momentum transfer in porous media: a theory of drying. Adv. Heat Transf. **13**(08), 119–203 (1977)